

Wirelessly Powered Crowd Sensing: Joint Power Transfer, Sensing, Compression, and Transmission

Xiaoyang Li, Changsheng You, Sergey Andreev, Yi Gong, and Kaibin Huang

Abstract

Leveraging massive numbers of sensors in user equipment as well as opportunistic human mobility, *mobile crowd sensing* (MCS) has emerged as a powerful paradigm, where prolonging battery life of constrained devices and motivating human involvement are two key design challenges. To address these, we envision a novel framework, named *wirelessly powered crowd sensing* (WPCS), which integrates MCS with *wireless power transfer* (WPT) for supplying the involved devices with extra energy and thus facilitating user incentivization. This paper considers a multiuser WPCS system where an *access point* (AP) transfers energy to multiple *mobile sensors* (MSs), each of which performs data sensing, compression, and transmission. Assuming lossless (data) compression, an optimization problem is formulated to simultaneously maximize data utility and minimize energy consumption at the operator side, by jointly controlling wireless-power allocation at the AP as well as sensing-data sizes, compression ratios, and sensor-transmission durations at the MSs. Given fixed compression ratios, the proposed optimal power allocation policy has the *threshold*-based structure with respect to a defined *crowd-sensing priority* function for each MS depending on both the operator configuration and the MS information. Further, for fixed sensing-data sizes, the optimal compression policy suggests that compression can reduce the total energy consumption at each MS only if the sensing-data size is sufficiently large. Our solution is also extended to the case of lossy compression, while extensive simulations are offered to confirm the efficiency of the contributed mechanisms.

This work was supported in part by Hong Kong Research Grants Council under the Grants 17209917 and 17259416, and Natural Science Foundation of Guangdong Province under Grant 2015A030313844.

X. Li, C. You and K. Huang are with the Dept. of EEE at The University of Hong Kong, Hong Kong (e-mail: lixy@eee.hku.hk, csyu@eee.hku.hk; huangk@eee.hku.hk). X. Li is also affiliated with the Dept. of EEE at Southern University of Science and Technology, Shenzhen, China.

S. Andreev is with the Laboratory of Electronics and Communications Engineering, Tampere University of Technology, Finland (e-mail: sergey.andreev@tut.fi).

Y. Gong is with the Dept. of EEE at Southern University of Science and Technology, Shenzhen, China (e-mail: gongy@sustc.edu.cn).

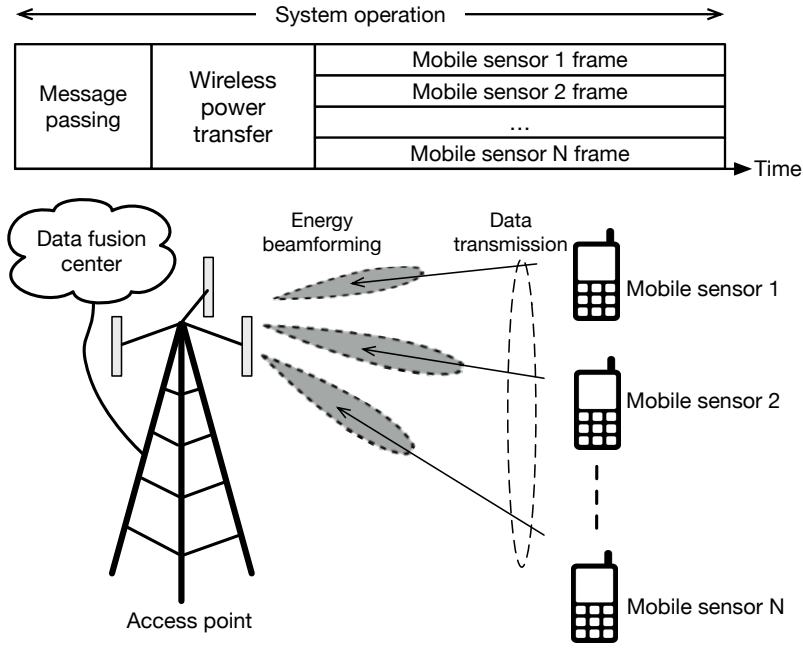


Figure 1: Our considered multiuser WPCS system.

I. INTRODUCTION

The unprecedented growth of the *Internet of Things* (IoT) applications for *Smart Cities* fuels the deployment of billions of wireless IoT devices that help automate a wide range of services, such as temperature measurement, pollution assessment, traffic monitoring, and public-safety surveillance. However, traditional *wireless sensor networking* (WSN) solutions are limited in their coverage and scalability, as well as suffer from high maintenance costs [1]. Recently, leveraging massive numbers of sensors in user handheld/wearable equipment led to the emergence of *mobile crowd sensing* (MCS), which is becoming a new paradigm that involves humans as part of the sensing infrastructure [2]. The key MCS challenges are prolonging device battery life and facilitating human engagement. These can be tackled by leveraging *wireless power transfer* (WPT) techniques as a user incentive for charging *mobile sensors* (MSs) within our proposed framework of *wirelessly powered crowd sensing* (WPCS) [3]. In this work, we consider a multiuser WPCS system in Fig. 1, which comprises an operator-deployed *access point* (AP) that transfers energy to multiple MSs. To optimize the operator's reward, we design a set of efficient control policies for maximizing data utility and minimizing energy consumption simultaneously.

A. Mobile Crowd Sensing

The consideration of MCS for IoT in Smart Cities has motivated research on advanced technologies that go beyond conventional WSNs, such as personal location-based systems, trusted sensing platforms, and people-centric sensing applications [2]. A key MCS design issue is *how to involve people into collaborate sensing*, as users may not be willing to contribute if the associated energy costs are high. There are two approaches to address this issue, known as *opportunistic* and *participatory* sensing [4], [5]. The former assumes that applications may run in the background and opportunistically collect data without user attention. The latter requires users to consciously participate in sensing activities and timely transmit the operator-requested data. However, this may consume significant device resources (i.e., battery and computing power), and it is essential to design incentivization mechanisms that compensate for the costs of participation [6]–[11].

Specifically, inspired by the location-based games, *entertainment as an incentive* was proposed in [7], which enriches the experience of participants who collect, e.g., geographic data on user preferences and interests. *Service as an incentive* is another widely-recognized mechanism. A typical example here is traffic monitoring, where users provide real-time traffic information (e.g., on road congestion) and in return receive timely services, such as accurate route planning. Finally, *money as an incentive* is an intuitive method that interprets sensed data as goods for gaining profit [8]. Accordingly, an auction scheme for MCS named reverse auction was proposed in [9], where the sellers (i.e., participants) submit their bidding prices to the buyer (i.e., operator) to compete for the data sensing activities. Further, the operator selects a subset of MSs for crowd sensing operation and determines individual payments. This approach was integrated with task labeling [10] by using Bayesian sequential learning to guarantee auction truthfulness, individual rationality, and budget feasibility.

In [11], the authors designed an alternative framework by utilizing Stackelberg game for monetary incentivization. The operator and the MSs negotiate in a two-stage manner to achieve the Stackelberg equilibrium: first the operator announces the payments and then each MS decides on whether to participate. Here, incentive allocation in multiuser MCS systems depends on the data quality of each user, which has been investigated in [12], [13]. In particular, the user data quality was estimated in [12] by using unsupervised learning techniques for characterizing long-term reputation. For privacy management, inverse correlation between the service quality and the privacy level was determined in [13] from the perspective of data analytics. Despite these substantial efforts, the issue of energy consumption at MSs is not yet resolved. The proposed work

addresses it by relying on advanced WPT techniques as well as contributes the first theoretical resource-allocation design of *trading energy for data*, which we envisioned in [3].

B. Wirelessly Powered Communication and Sensing

Designed originally for point-to-point power transmission, the WPT technology has already comprised advanced techniques from inductive coupling and electromagnetic radiation [14], [15]. Further integration of information and power transmission gave rise to the emerging field of *simultaneous wireless information and power transfer* (SWIPT) [16]. Multiple works focused on applying SWIPT to a variety of communication systems and networks, including two-way transmission [17], relaying [18]–[20], *multiple-input-multiple-output* (MIMO) communication [16], *orthogonal frequency division multiple access* (OFDMA) transmission [21], and cognitive networking [22], among others. Further design efforts tailored it for practical setups by accounting for channel state information [23] and quality of service considerations [24]. Recently, WPT was considered for *unmanned aerial vehicles* (UAVs) [25] and mobile-edge computing networks [26] for powering computation offloading in energy-constrained devices.

Another important application of WPT is in sensing systems, where the MSs have limited energy storage due to their compact form-factor, but are expected to perform sophisticated sensing tasks cooperatively. Powering these sensors is a challenge since frequent battery recharging/replacement is impractical if not impossible. Recent breakthroughs in WPT techniques offer a viable solution by powering MSs with energy beamforming [27]–[31]. Specifically, a multi-antenna *wirelessly powered sensor networking* (WPSN) testbed has been developed in [28], where a power beacon transfers energy to a sensor node via an adaptive energy-beamforming scheme. For multiple WPSN sensors, design of energy beamforming is much more convoluted. In [29], accounting for practical sensing and circuit power consumption at MSs, the authors proposed a collaborative energy-beamforming scheme for powering a cluster of sensors to transfer data by using distributed information beamforming. Cooperative sensing was further addressed in [30], where clusters of sensors forward their information by utilizing relay and SWIPT techniques. Finally, for low-complexity passive backscatter sensors, a novel architecture for large-scale WPSN systems was recently proposed in [31], where the sensors are powered by distributed power beacons. However, the existing literature concentrates on optimizing WPT efficiency to improve the sensing-and-communication throughput, but disregards design of incentivization schemes and operator's reward. In this work, we bridge this gap by integrating WPT with MCS

to facilitate human involvement into collective sensing activities, thus simultaneously maximizing data utility and minimizing energy consumption at the operator side.

C. Contribution and Organization

In this work, by leveraging the potential of WPT for powering MSs and motivating MCS, we aim at addressing the following two key issues.

- The first one is *how to incentivize and select MSs* for crowd-sensing operation. This includes designing a new incentivization approach that can trade energy for data depending on the data utility at different MSs. An optimized sensor selection policy needs to be developed at the operator to select a set of sensors to participate in the MCS for maximum reward.
- The second one is *how to jointly control wireless-power allocation, data sensing, compression, and transmission* at the selected MSs. This requires the operator to allocate wireless power for improved energy supply of each MS, and the MSs should employ energy-efficient sensing, compression, and transmission policies to minimize the energy consumption.

To account for these two considerations, this paper considers a multiuser WPCS system controlled by an operator and comprising a multiple-antenna AP that transfers energy to multiple single-antenna MSs. Each MS accumulates a part of such energy as a reward and utilizes the rest to conduct the MCS tasks, including sensing, data compression, and transmission of compressed data to the AP. We consider both lossless and lossy (data) compression as well as design a joint control policy for maximizing data utility and minimizing energy consumption at the AP simultaneously. The main contributions of this work are summarized as follows.

- *Problem formulation and iterative solution:* For lossless compression, we formulate an optimization problem for simultaneously maximizing data utility and minimizing energy consumption at the operator. An iterative solution that reaches the local optimum is proposed for the joint optimization of power allocation, sensing, compression, and transmission.
- *Joint Optimization of Power Allocation, Sensing, and Transmission:* Given fixed compression ratios, the considered non-convex problem is reduced to a convex formulation. We first derive a semi-closed form expression for the optimal sensor-transmission duration. The results are used for deriving the optimal wireless-power allocation and sensing-data sizes.
- *Joint Optimization of Compression and Transmission:* Given fixed sensing-data sizes, the sensor-transmission durations and compression ratios are optimized for minimizing energy

consumption at the operator. The derived optimal policy suggests that the MSs should perform data compression only if the sensing-data size exceeds a certain threshold.

- *Optimal control for lossy compression:* The proposed solution is also extended to lossy compression, where the optimization problem is modified to account for the respective data utility degradation. Given fixed compression ratios, the corresponding approach is similar to the lossless case. For the second sub-problem, to preserve the data utility, we further optimize both sensing-data sizes and compression ratios at the MSs.

The rest of this paper is organized as follows. The system model is introduced in Section II. Section III studies efficient joint control in the WPCS system based on lossless compression. In Section IV, this approach is extended for the system with lossy compression. The simulation results are offered in Section V, followed by the conclusions in Section VI.

II. SYSTEM MODEL

Consider a multiuser WPCS system shown in Fig. 1 comprising multiple single-antenna MSs and one multi-antenna AP. The model of system operation is described in the sub-sections.

A. WPCS Operation

We focus on a particular fixed time window for crowd-sensing, which is divided into three phases: *message passing*, *WPT*, and *crowd sensing* (see Fig. 1).

Consider the *message-passing phase*. Each sensor feeds back to the AP its parameters including channel gain, sensing, and compression power. Given the knowledge of all sensors' parameters, the AP jointly optimizes the power allocation for WPT and sensor operations (namely, data sensing, compression, and transmission). The objective is to simultaneously maximize data utility and minimize energy consumption (see the performance metric in the sequel). Subsequently, the AP informs individual sensors on their allocated power, optimal compression ratios, sensing-data sizes, and time partitions for sensing, compression, and transmission.

Next, in the *WPT phase*, the AP uses an antenna array to beam energy to the MSs as an incentive for sensing (see Fig. 1). Upon harvesting energy, each MS stores part of the energy as a reward and applies the rest to operate the sensing tasks including sensing, data compression, and transmission of compressed data to the AP.

Last, in the *crowd-sensing phase*, the sensors simultaneously perform data sensing, compression, and transmission based on the settings determined by the AP in the message-passing phase.

The parallel data collection is enabled by transmissions over orthogonal channels allocated by the AP to sensors. The time duration for crowd sensing, denoted as T , is divided into three slots with *adjustable* durations $t_n^{(s)}$, $t_n^{(c)}$, and t_n , which are used for sensing, compression, and transmission, respectively. This introduces the following constraint:

$$\text{(Time constraint)} \quad t_n^{(s)} + t_n^{(c)} + t_n \leq T. \quad (1)$$

B. Model of Wireless Power Transfer

In the WPT phase with a fixed duration of T_0 (second), the AP transfers energy simultaneously to N MSs by pointing N radio beams to the corresponding MSs. Let h_n denote the effective channel gain between the AP and MS n , and P_n the transmission power of the corresponding beam. The AP transmission power is assumed to be fixed and represented by P_0 , resulting in the following constraint:

$$\text{(Power constraint)} \quad \sum_{n=1}^N P_n \leq P_0. \quad (2)$$

The energy transferred from the AP to MS n , denoted by $E_n^{(h)}(P_n)$, is $E_n^{(h)}(P_n) = \eta P_n h_n T_0$, where the constant $0 < \eta < 1$ represents the energy conversion efficiency.

Each of the sensors selected to participate in crowd sensing stores part of received energy as the reward. Let the reward energy at sensor n , denoted by $E_n^{(r)}(\ell_n^{(s)})$, be proportional to the size of sensing data, namely, $E_n^{(r)}(\ell_n^{(s)}) = q_n^{(r)} \ell_n^{(s)}$ with $q_n^{(r)}$ being a fixed scaling factor. The remaining energy, $(E_n^{(h)} - E_n^{(r)})$, is consumed by the sensor operations including sensing, compression, and transmission, where energy consumption is represented respectively by $E_n^{(s)}$, $E_n^{(c)}$, and $E_n^{(t)}$ and specified in the sequel. Based on the above discussion, the power constraint in (2) leads to the following energy constraint:

$$\text{(Energy constraint)} \quad \sum_{n=1}^N (E_n^{(r)} + E_n^{(s)} + E_n^{(c)} + E_n^{(t)}) \leq \eta h_n P_0 T_0. \quad (3)$$

C. Mobile-Sensor Model

At each MS, crowd sensing comprises three sequential operations: data sensing, data compression, and data transmission, as shown in Fig. 2 and modeled as follows.

1) *Data sensing model:* Consider MS n . Let s_n denote the output data rate. Given the sensing time-duration $t_n^{(s)}$, the size of raw sensing data, denoted by $\ell_n^{(s)}$ (bit), is $\ell_n^{(s)} = s_n t_n^{(s)}$. Let $q_n^{(s)}$ denote the sensing energy consumption for generating 1-bit of data. The total energy consumption for sensing at MS n , denoted as $E_n^{(s)}(\ell_n^{(s)})$, is given as $E_n^{(s)}(\ell_n^{(s)}) = q_n^{(s)} \ell_n^{(s)}$.

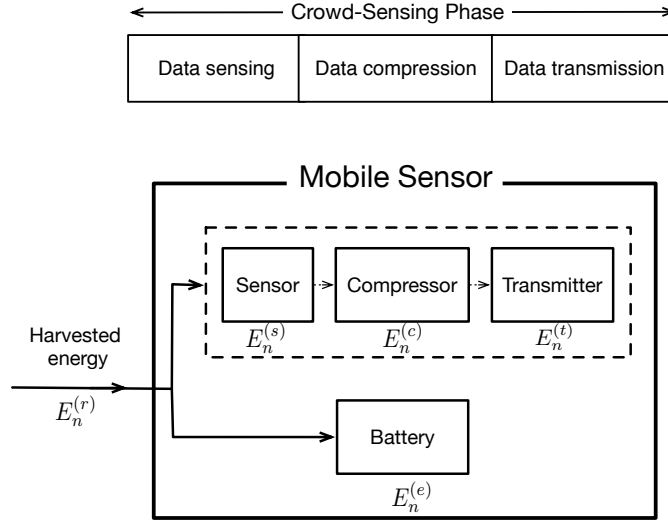


Figure 2: Mobile sensor architecture, operation, and energy consumption.

2) *Data compression model*: First, consider lossless compression of sensed data, for which the original data can be perfectly reconstructed from the compressed data. Relevant techniques include Huffman, run-length, and Lempel-Ziv encoding. It is assumed that all MSs deploy the same lossless compression method with the maximum *compression ratio*, denoted as R_{\max} , namely, the maximum ratio between the sizes of raw and compressed data. Let $R_n \in [1, R_{\max}]$ denote the compression ratio chosen by MS n . Then the size of compressed data ℓ_n is given as $\ell_n = \ell_n^{(s)} / R_n$. Note that in the current literature, there is still a lack of well established model for the computation complexity of data compression. However, a tractable model can be inferred from existing measurement results for Zlib compression [32]. Specifically, the required CPU cycles for compressing 1-bit of data can be approximated as an exponential function of the compression ratio R_n as:

$$\text{(Compression complexity)} \quad C(R_n, \epsilon) = e^{\epsilon R_n} - e^{\epsilon}, \quad (4)$$

where ϵ is a positive constant depending on the compression method. At $R_n = 1$, $C(R_n, \epsilon) = 0$, which corresponds to no compression. Let f_n denote the fixed CPU-cycle frequency at MS n and $t_n^{(c)}$ is the compression time duration. Then $t_n^{(c)} = (\ell_n^{(s)} C(R_n, \epsilon)) / f_n$. Following the practical model in [33], each CPU cycle consumes energy of $q_n^{(c)} = \alpha f_n^2$ where α is a constant determined by the circuits. The energy consumption for data compression at MS n , denoted by $E_n^{(c)}(\ell_n^{(s)}, R_n)$, is given as $E_n^{(c)}(\ell_n^{(s)}, R_n) = q_n^{(c)} \ell_n^{(s)} C(R_n, \epsilon)$ with $C(R_n, \epsilon)$ in (4). It follows that

$$\text{(Compression energy)} \quad E_n^{(c)}(\ell_n^{(s)}, R_n) = q_n^{(c)} \ell_n^{(s)} (e^{\epsilon R_n} - e^{\epsilon}). \quad (5)$$

Next, consider lossy compression that achieves a larger compression ratio than its lossless counterpart at the cost of information loss. Typical techniques involve data truncation after a transform (e.g., discrete cosine transform), or by discarding data insensitive for users' perception. Our model of compression energy consumption follows that in (5) with the parameters $\{R_n, R_{\max}, \epsilon\}$ replaced by their counterparts for lossy compression $\{\bar{R}_n, \bar{R}_{\max}, \bar{\epsilon}\}$. The information loss can be measured by the *quality factor*, denoted by $b_n \in (0, 1]$, defined as the equivalent size of raw data for 1-bit of compressed data in terms of utility. The quality factor, however, has not been well modeled in the existing literature. To address it, one tractable model can be inferred from the simulation results in [34], given by $b_n = 1/\sqrt{\bar{R}_n}$. Specifically, $b_n \rightarrow 0$ when $\bar{R}_n \rightarrow \infty$, and $b_n \rightarrow 1$ when $\bar{R}_n \rightarrow 1$, which corresponds to no compression.

3) *Data transmission model*: Each selected MS transmits compressed data to the AP. Let $P_n^{(t)}$ denote the transmission power and t_n is the transmission time duration. Assuming channel reciprocity, the achievable transmission rate (in bit/s), denoted by v_n , can be given as $v_n = \ell_n/t_n = B \log_2(1 + \frac{h_n P_n^{(t)}}{N_0})$ where B is the bandwidth and N_0 is the variance of complex-white-Gaussian noise. As such, the transmission energy consumption denoted by $E_n^{(t)}(\ell_n)$ follows: $E_n^{(t)}(\ell_n) = P_n^{(t)} t_n = \frac{t_n}{h_n} f(\ell_n/t_n)$ where the function $f(x)$ is defined as $f(x) = N_0(2^{\frac{x}{B}} - 1)$.

4) *Time and energy constraints (revisited)*: Last, based on the above models, the time constraint in (1) and energy constraint in (3) can be rewritten as

$$\text{(Time constraint)} \quad \frac{\ell_n^{(s)}}{s_n} + \frac{\ell_n^{(s)} C(R_n, \epsilon)}{f_n} + t_n \leq T, \quad (6)$$

$$\text{(Energy constraint)} \quad [q_n^{(r)} + q_n^{(s)} + q_n^{(c)} C(R_n, \epsilon)] \ell_n^{(s)} + \frac{t_n}{h_n} f\left(\frac{\ell_n^{(s)}}{t_n R_n}\right) \leq \eta h_n P_n T_0. \quad (7)$$

An important observation from the time constraint is that given the sensing rate s_n and CPU-cycle frequency f_n , the partitioning of crowd-sensing time of sensor n for sensing, compression, and transmission can be determined by the *sensing-data size* ℓ_n , *compression ratio* R_n , and *transmission time* t_n to be optimized in the sequel.

D. Performance Metrics

Recall that the *operator's reward*, which is our performance metric, refers to the difference between the sum weighted data utility and weighted energy cost. Its mathematical definition is provided as follows. Following a commonly used model (see e.g., [35]), the utility of ℓ_n -bit data delivered by sensor n is measured by the logarithmic function $a_n \log(1 + b_n \ell_n^{(s)})$ where b_n is

the mentioned information loss due to compression and a_n is a weight factor depending on the type of data. Note that the logarithmic function is chosen to model the diminishing return as the data size increases. Hence, the sum data utility for the operator, denoted by $U(\ell_n^{(s)})$, is

$$U(\ell_n^{(s)}) = \sum_{n=1}^N a_n \log(1 + b_n \ell_n^{(s)}). \quad (8)$$

Then the operator's reward, denoted by $R(\ell_n^{(s)}, P_n)$, can be modeled as

$$R(\ell_n^{(s)}, P_n) = \sum_{n=1}^N a_n \log(1 + b_n \ell_n^{(s)}) - c \sum_{n=1}^N P_n T_0, \quad (9)$$

where c denotes the price of unit energy with respect to that of unit data utility.

III. JOINT POWER ALLOCATION, SENSING, COMPRESSION, AND TRANSMISSION

In this section, we formulate and solve the problem of jointly optimizing power allocation, sensing, lossless compression, and transmission as discussed in Section II. This yields the optimal policy and guidelines for operating the proposed WPCS system. The results are extended to the case of lossy compression in the next section.

A. Problem Formulation

The specific design problem here is to jointly optimize the AP power allocation for WPT to sensors, $\{P_n\}$, the sizes of sensing data, $\{\ell_n^{(s)}\}$, the data compression ratios, $\{R_n\}$, and the partitioning of crowd-sensing time for sensing and compression, determined by $\{t_n\}$ together with $\{\ell_n^{(s)}\}$ and $\{R_n\}$. The objective is to maximize the operator's reward in (9) under the power constraint in (2), time constraint in (6), and energy constraint in (7). Mathematically, the optimization problem can be formulated as follows:

$$\begin{aligned}
 & \max_{\substack{P_n \geq 0, \ell_n^{(s)} \geq 0, \\ R_n \in [1, R_{\max}], t_n \geq 0}} && \sum_{n=1}^N a_n \log(1 + \ell_n^{(s)}) - c \sum_{n=1}^N P_n T_0 \\
 & \text{s.t.} && \sum_{n=1}^N P_n \leq P_0, \\
 \text{(P1)} && \frac{\ell_n^{(s)}}{s_n} + \frac{\ell_n^{(s)} C(R_n, \epsilon)}{f_n} + t_n \leq T, && n = 1, \dots, N, \\
 && [q_n^{(r)} + q_n^{(s)} + q_n^{(c)} C(R_n, \epsilon)] \ell_n^{(s)} + \frac{t_n}{h_n} f \left(\frac{\ell_n^{(s)}}{t_n R_n} \right) \leq \eta P_n h_n T_0, && n = 1, \dots, N.
 \end{aligned}$$

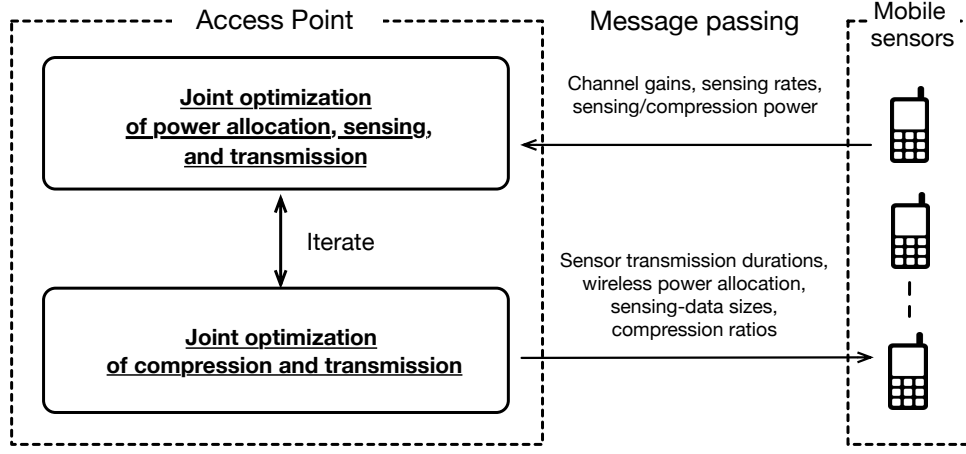


Figure 3: Implementation of our iterative solution for optimal WPCS.

B. Iterative Solution Approach

First, the convexity of problem P1 is characterized as follows.

Lemma 1. Problem P1 is a *non-convex* optimization problem.

This lemma can be easily proved since the optimization variables, $\{\ell_n^{(s)}, R_n, t_n\}$, are coupled at the constraints in forms of $\ell_n^{(s)} C(R_n, \epsilon)$ and $\frac{t_n}{h_n} f\left(\ell_n^{(s)} / (t_n R_n)\right)$. To establish an optimal policy for attaining a local maximum and characterize its structure, we propose an *iterative* solution approach as shown in Fig. 3. Specifically, the approach iterates between solving two sub-problems, P1-A and P1-B given below, for optimizing two subsets of parameters, namely, $\{P_n, \ell_n^{(s)}, t_n\}$ and $\{R_n, t_n\}$, respectively. The reason for such separation of parametric optimization is that it creates two convex sub-problems as shown in the sequel. It is necessary to include the transmission durations $\{t_n\}$ as variables in both sub-problems since they are affected by all other parameters. First, with the compression ratios $\{R_n\}$ fixed, problem P1 reduces to the following problem P1-A, named *joint optimization of power allocation, sensing, and transmission*:

$$\begin{aligned}
 \text{(P1-A)} \quad & \max_{P_n \geq 0, \ell_n^{(s)} \geq 0, t_n \geq 0} \quad \sum_{n=1}^N a_n \log(1 + \ell_n^{(s)}) - c \sum_{n=1}^N P_n T_0 \\
 & \text{s.t.} \quad \sum_{n=1}^N P_n \leq P_0, \\
 & \quad \beta_n \ell_n^{(s)} + t_n \leq T, \quad n = 1, \dots, N, \\
 & \quad \alpha_n \ell_n^{(s)} + \frac{t_n}{h_n} f\left(\frac{\ell_n^{(s)}}{R_n t_n}\right) \leq \eta P_n h_n T_0, \quad n = 1, \dots, N,
 \end{aligned}$$

where $\alpha_n = q_n^{(r)} + q_n^{(s)} + q_n^{(c)}C(R_n, \epsilon)$ and $\beta_n = \frac{1}{s_n} + \frac{C(R_n, \epsilon)}{f_n}$. Next, given the parameters $\{P_n\} \cup \{\ell_n^{(s)}\} \cup \{t_n\}$, the sensing-data sizes $\ell_n^{(s)}$ are fixed and thus problem P1 is reduced to the minimization of sum energy consumption: $\sum_{n=1}^N P_n T_0$. Given this criterion, the energy constraints in (7) are active at the optimal point:

$$\left[q_n^{(r)} + q_n^{(s)} + q_n^{(c)}C(R_n, \epsilon) \right] \ell_n^{(s)} + \frac{t_n}{h_n} f \left(\frac{\ell_n^{(s)}}{t_n R_n} \right) = \eta P_n h_n T_0. \quad (10)$$

By substituting this, the problem P1-B, named *joint optimization of compression and transmission*, can be produced from problem P1 as:

$$\begin{aligned} \text{(P1-B)} \quad & \min_{1 \leq R_n \leq R_{\max}, t_n \geq 0} && q_n^{(r)} \ell_n^{(s)} + q_n^{(s)} \ell_n^{(s)} + q_n^{(c)} \ell_n^{(s)} C(R_n, \epsilon) + \frac{t_n}{h_n} f \left(\frac{\ell_n^{(s)}}{t_n R_n} \right) \\ & \text{s.t.} && \frac{\ell_n^{(s)}}{s_n} + \frac{\ell_n^{(s)} C(R_n, \epsilon)}{f_n} + t_n \leq T. \end{aligned}$$

By iteratively solving these two problems, which are proved to be convex in the sequel, the solution is guaranteed to converge and reach a local maximum of the operator's reward function in formulation P1.

C. Joint Optimization of Power Allocation, Sensing, and Transmission

To solve problem P1-A, we first prove that it can be reduced to the problem of transmission-duration optimization. Then the solution of the reduced problem is used to characterize the optimal wireless power allocation and sensing-data sizes.

1) *Optimal Sensor Transmission:* Problem P1-A is solved as follows. First, we observe that problem P1-A is always feasible since $\{P_n = 0, \ell_n^{(s)} = 0, R_n = 1\}$ for each n is a feasible solution. Next, some useful necessary conditions for the optimal solution are provided as follows.

Lemma 2. As a result of solving problem P1-A, the optimal power allocation $\{P_n^*\}$, sensor transmission durations $\{t_n^*\}$, and sensing-data sizes $\{(\ell_n^{(s)})^*\}$ satisfy the following:

$$\alpha_n (\ell_n^{(s)})^* + \frac{t_n^*}{h_n} f \left(\frac{(\ell_n^{(s)})^*}{R_n t_n^*} \right) = \eta P_n^* h_n T_0, \quad \text{and} \quad \beta_n (\ell_n^{(s)})^* + t_n^* = T, \quad \forall n. \quad (11)$$

Lemma 2 is proved in Appendix A. The equalities arise from the fact that to maximize the operator's reward, each MS should *fully* utilize the transferred energy and the crowd-sensing time duration. Based on these equalities, $\{P_n^*\}$ and $\{(\ell_n^{(s)})^*\}$ can be written as functions of $\{t_n^*\}$.

Consequently, problem P1-A can be equivalently transformed into problem P2 for sensor-duration optimization having only $\{t_n\}$ as the variables:

$$\begin{aligned}
 \text{(P2)} \quad & \max_{t_n \geq 0} \quad \sum_{n=1}^N a_n \log \left(1 + \frac{T - t_n}{\beta_n} \right) - c \sum_{n=1}^N \left[\frac{\alpha_n(T - t_n)}{\eta \beta_n h_n} + \frac{t_n}{\eta h_n^2} f \left(\frac{T - t_n}{R_n \beta_n t_n} \right) \right] \\
 \text{s.t.} \quad & \sum_{n=1}^N \left[\frac{\alpha_n(T - t_n)}{\eta \beta_n h_n} + \frac{t_n}{\eta h_n^2} f \left(\frac{T - t_n}{R_n \beta_n t_n} \right) \right] \leq P_0 T_0, \quad n = 1, \dots, N, \\
 & 0 \leq t_n \leq T, \quad n = 1, \dots, N.
 \end{aligned}$$

The convexity of problem P2 is established in the following lemma, which can be easily proved by showing that the objective is a concave function and the inequality constraints are convex constraints, omitted for brevity.

Lemma 3. Problem P2 is a convex optimization problem.

As a result, problem P2 can be solved by the Lagrange method. The corresponding partial Lagrange function is

$$L(t_n, \lambda) = \sum_{n=1}^N \left[(\lambda + c) \left(\frac{\alpha_n(T - t_n)}{\eta \beta_n h_n} + \frac{t_n}{\eta h_n^2} f \left(\frac{T - t_n}{R_n \beta_n t_n} \right) \right) - a_n \log \left(1 + \frac{T - t_n}{\beta_n} \right) \right] - \lambda P_0 T_0. \quad (12)$$

Define a function $y(x)$ as $y(x) = f(x) - (x + \frac{1}{R_n \beta_n})f'(x)$ and t_n^* as the optimal solution for solving problem P2. Then applying *Karush-Kuhn-Tucker* (KKT) conditions leads to the following necessary and sufficient conditions:

$$\frac{\partial L}{\partial t_n^*} = \frac{a_n}{\beta_n + (T - t_n^*)} + \frac{(\lambda^* + c_n)}{\eta h_n} \left[\frac{1}{h_n} y \left(\frac{T - t_n^*}{R_n \beta_n t_n^*} \right) - \frac{\alpha_n}{\beta_n} \right] \begin{cases} > 0, & t_n^* = 0, \\ = 0, & 0 < t_n^* < T, \\ < 0, & t_n^* = T, \end{cases} \quad (13a)$$

$$\lambda^* \left(\sum_{n=1}^N \left[\frac{t_n^*}{\eta h_n^2} f \left(\frac{T - t_n^*}{R_n \beta_n t_n^*} \right) + \frac{\alpha_n(T - t_n^*)}{\eta \beta_n h_n} \right] - P_0 T_0 \right) = 0. \quad (13b)$$

Combing these conditions yields the optimal sensor-transmission policy given as follows.

Proposition 1 (Optimal Sensor Transmission). Given fixed compression ratios, for each MS selected for crowd sensing with $(0 < t_n^* \leq T)$, the optimal transmission duration t_n^* satisfies:

$$\frac{a_n}{\beta_n + (T - t_n^*)} + \frac{(\lambda^* + c)N_0}{\eta h_n^2} \left[\left(1 - \frac{T \ln 2}{B R_n \beta_n t_n^*} \right) 2^{\frac{T - t_n^*}{B R_n \beta_n t_n^*}} - 1 \right] - \frac{(\lambda^* + c)\alpha_n}{\eta h_n \beta_n} = 0, \quad (14)$$

where λ^* satisfies the condition in (13b).

Algorithm 1 A Bisection-Search Algorithm for Computing the Optimal Sensor Transmission

- **Step 1** [Initialize]: Let $\lambda_\ell = 0$, $\lambda_h = \lambda_{\max}$, $\varepsilon > 0$.
 Obtain $t_{n,\ell}$ and $t_{n,h}$ based on (14), calculate $E_\ell = \sum_{n=1}^N \left[\frac{\alpha_n(T-t_{n,\ell})}{\eta\beta_n h_n} + \frac{t_{n,\ell}}{\eta h_n^2} f\left(\frac{T-t_{n,\ell}}{R_n\beta_n t_{n,\ell}}\right) \right]$ and $E_h = \sum_{n=1}^N \left[\frac{\alpha_n(T-t_{n,h})}{\eta\beta_n h_n} + \frac{t_{n,h}}{\eta h_n^2} f\left(\frac{T-t_{n,h}}{R_n\beta_n t_{n,h}}\right) \right]$ respectively.
 - **Step 2** [Bisection search]: While $E_\ell \neq P_0 T_0$ and $E_h \neq P_0 T_0$, update λ_ℓ and λ_h as follows.
 - (1) Define $\lambda_m = (\lambda_\ell + \lambda_h)/2$, compute $t_{n,m}$ and $E_m = \sum_{n=1}^N \left[\frac{\alpha_n(T-t_{n,m})}{\eta\beta_n h_n} + \frac{t_{n,m}}{\eta h_n^2} f\left(\frac{T-t_{n,m}}{R_n\beta_n t_{n,m}}\right) \right]$.
 - (2) If $E_m < P_0 T_0$, let $\lambda_h = \lambda_m$, else $\lambda_\ell = \lambda_m$.
 Until $\lambda_h - \lambda_\ell < \varepsilon$. Return $t_n^* = t_{n,m}$.
-

One can observe from Proposition 1 that the optimal sensor-transmission duration t_n^* has no closed form. However, the value of t_n^* can be efficiently computed using the proposed bisection-search procedure presented in Algorithm 1. Based on Proposition 1, the dependence of the optimal sensor-transmission durations on the utility weights and channels is characterized in the following corollary.

Corollary 1 (Properties of Optimal Sensor Transmission). The optimal sensor-transmission durations $\{t_n^*\}$ have the following properties:

- 1) If the channel gains $\{h_n\}$ are identical but the utility weights satisfy $a_1 \geq a_2 \cdots \geq a_N$, then $t_1^* \leq t_2^* \cdots \leq t_N^*$.
- 2) If the utility weights $\{a_n\}$ are identical but the channel gains satisfy $h_1 \geq h_2 \cdots \geq h_N$, then $t_1^* \leq t_2^* \cdots \leq t_N^*$.

The proof is given in Appendix B. These cases indicate that for a sensor with large utility weight and high channel gain, it is beneficial to have a short transmission duration so that the sensing duration can be longer to increase the amount of sensing data, for larger sum data utility.

Last, the following result for the case of small optimal transmission durations ($t_n^* \ll T$) follows from Proposition 1 by substituting $T - t_n^* \approx T$.

Corollary 2 (Approximate Optimal Sensor Transmission). Consider the optimal sensor-transmission duration t_n^* in (14). If $t_n^* \ll T$,

$$t_n^* \approx \frac{T \ln 2}{\tilde{\theta}}, \quad (15)$$

where $\tilde{\theta} = BR_n\beta_n \left[W_0 \left(\left(\frac{a_n \eta h_n^2}{(c + \lambda^*)(\beta_n + T)N_0} - \frac{h_n \alpha_n}{N_0 \beta_n} - 1 \right) e^{\frac{\ln 2}{BR_n\beta_n} - 1} \right) + 1 \right]$.

First of all, one can observe that the approximate result retains the properties in Corollary 1. Moreover, this result shows that the optimal sensor-transmission duration increases with the growing sensing-and-compression power represented by α_n defined in problem P1-A.

2) *Optimal Wireless-Power Allocation:* Combining the optimal sensor-transmission policy in Proposition 1 and optimality conditions in Lemma 2 yields the optimal wireless-power allocation policy shown in the following proposition, which is proved in Appendix C.

Proposition 2 (Optimal Wireless-Power Allocation). The optimal wireless-power allocation policy $\{P_n^*\}$ that solves problem P1-A is given as

$$P_n^* = \begin{cases} \frac{1}{h_n \eta T_0} \left[\frac{t_n^*}{h_n} f\left(\frac{T - t_n^*}{R_n \beta_n t_n^*}\right) + \frac{\alpha_n (T - t_n^*)}{\beta_n} \right], & \varphi_n \geq \lambda^*, \\ 0, & \varphi_n < \lambda^*, \end{cases} \quad (16)$$

where t_n^* and λ^* are given in Proposition 1, and φ_n is named the *crowd-sensing priority function* defined as

$$\varphi_n = \kappa_n - c \quad \text{with} \quad \kappa_n \triangleq \frac{a_n \eta h_n}{q_n^{(r)} + q_n^{(s)} + q_n^{(c)} C(R_n, \epsilon) + \frac{N_0 \ln 2}{h_n B R_n}}. \quad (17)$$

Proposition 2 shows that the optimal wireless-power allocation policy has a *threshold*-based structure. In other words, only the MSs with (crowd-sensing) priority functions exceeding the threshold λ^* will be allocated wireless power or equivalently selected for participating in the crowd sensing. Specifically, both the operator's configuration (including cost weight as well as provisioned power), and MSs' individual parameters significantly affect the crowd-sensing sensor selection as discussed in the following remarks.

Remark 1 (Effects of Operator's Configuration on Sensor Selection). First, it can be observed from (17) that if the cost weight c is sufficiently large ($c > \max\{\kappa_n\}$), the priority function for each sensor is negative, i.e., $\varphi_n \leq 0, \forall n$. Since the Lagrange multiplier $\lambda^* \geq 0$, it follows that $\varphi_n < \lambda^*, \forall n$, implying that no sensor is selected for crowd sensing. On the other hand, if the energy cost is negligible (i.e., $c = 0$), each sensor has a positive priority function. In this case, provided that the operator supplies sufficient power for crowd sensing thus leading to $\lambda^* = 0$ (see (13a)), all the sensors will be selected to participate in the crowd sensing to increase the operator's reward. For the general case of finite c and $\lambda^* > 0$, it is desirable for the operator to choose only a subset of sensors with priorities above λ^* for crowd sensing.

Remark 2 (Effects of Sensor Parameters on Sensor Selection). Individual parameters of sensors also affect the sensor-selection policy by the term of κ_n defined in (17). To be specific, the sensor with smaller sensing-and-compression power and a larger channel gain has higher crowd-sensing priority and thus is more likely to be selected for crowd sensing. Such sensors with larger channel gains can not only harvest more energy, but also consume less transmission power for data transmission. Last, to compete for crowd sensing with other sensors, a sensor can reduce its amount of reward power, $q_n^{(r)}$, so as to increase its own priority function.

Finally, the sum allocated power is affected by the cost weight as shown below.

Corollary 3. The sum allocated power $\sum_{n=1}^N P_n^* T_0$ decreases with the cost weight c . In particular, $\sum_{n=1}^N P_n^* T_0 = P_0 T_0$, if $c = 0$.

This corollary is aligned with intuition and suggests that the optimal wireless power allocation balances the tradeoff between obtaining data utility and energy with the price measured by c .

3) *Optimal Sensing-Data Sizes:* Using a similar approach for deriving the optimal wireless power allocation in Proposition 2, the optimal sensing-data sizes can be derived in the following proposition by using Proposition 1 and Lemma 2.

Proposition 3 (Optimal Sensing-Data Sizes). The optimal sensing-data sizes $\{(\ell_n^{(s)})^*\}$ that solve problem P1-A are given as:

$$(\ell_n^{(s)})^* = \begin{cases} \frac{T - t_n^*}{\beta_n}, & \varphi_n \geq \lambda^*, \\ 0, & \varphi_n < \lambda^*, \end{cases} \quad (18)$$

where t_n^* and λ^* are given in Proposition 1, and φ_n is defined in (17).

The effects of parameters on the sensing-data size are characterized as follows.

Corollary 4 (Properties of Optimal Sensing-Data Sizes). The optimal sensing-data sizes $\{(\ell_n^{(s)})^*\}$ have the following properties:

- 1) If the channel gains $\{h_n\}$ are identical but the utility weights satisfy $a_1 \geq a_2 \cdots \geq a_N$, then $(\ell_1^{(s)})^* \geq (\ell_2^{(s)})^* \cdots \geq (\ell_N^{(s)})^*$.
- 2) If the utility weights $\{a_n\}$ are identical but the channel gains satisfy $h_1 \geq h_2 \cdots \geq h_N$, then $(\ell_1^{(s)})^* \geq (\ell_2^{(s)})^* \cdots \geq (\ell_N^{(s)})^*$.

This corollary reflects the intuition that it is desirable to increase the sensing-data sizes for sensors with high channel gains since they consume less transmission energy.

D. Joint Optimization of Compression and Transmission

Consider the optimization problem formulated in problem P1-B (see Section III-B). First, the problem convexity is established in the following lemma, which can be easily proved by using the property of *perspective function* [36].

Lemma 4. Problem P1-B is a convex optimization problem.

Hence, problem P1-B can be solved by the Lagrange method. The Lagrange function is

$$\hat{L}(R_n, t_n, \hat{\lambda}) = Q(R_n)\ell_n^{(s)} + \frac{t_n}{h_n}f\left(\frac{\ell_n^{(s)}}{t_n R_n}\right) + \hat{\lambda}\left(t_n + \frac{\ell_n^{(s)}C(R_n, \epsilon)}{f_n} + \frac{\ell_n^{(s)}}{s_n} - T\right), \quad (19)$$

where $Q(R_n) = q_n^{(r)} + q_n^{(s)} + q_n^{(c)}C(R_n, \epsilon)$. Let $g(x) = f(x) - xf'(x)$ and t_n^*, R_n^* are the optimal solution for solving problem P1-B. Directly applying KKT conditions results in the following necessary and sufficient conditions:

$$\frac{\partial \hat{L}}{\partial R_n^*} = \left(q_n^{(c)} + \frac{\hat{\lambda}^*}{f_n}\right)\ell_n^{(s)}\epsilon e^{\epsilon R_n^*} - \frac{\ell_n^{(s)}}{h_n R_n^{*2}}f'\left(\frac{\ell_n^{(s)}}{t_n^* R_n^*}\right) \begin{cases} > 0, & R_n^* = 1, \\ = 0, & 1 < R_n^* < R_{\max}, \\ < 0, & R_n^* = R_{\max}, \end{cases} \quad (20a)$$

$$\frac{\partial \hat{L}}{\partial t_n^*} = \frac{1}{h_n}g\left(\frac{\ell_n^{(s)}}{t_n^* R_n^*}\right) + \hat{\lambda}^* \begin{cases} > 0, & t_n^* = 0, \\ = 0, & 0 < t_n^* < T, \\ < 0, & t_n^* = T, \end{cases} \quad (20b)$$

$$\hat{\lambda}^* \left(t_n^* + \frac{\ell_n^{(s)}C(R_n, \epsilon)}{f_n} + \frac{\ell_n^{(s)}}{s_n} - T\right) = 0. \quad (20c)$$

Then the optimal sensor decisions on *compress-or-not* follow.

Lemma 5 (Compress-or-Not?). Given fixed sensing-data sizes, sensor n should perform data compression (i.e., $R_n < 1$) for minimizing its energy consumption, if and only if its sensing-data size satisfies:

$$\ell_n^{(s)} > \frac{T}{\hat{\theta}}, \text{ where } \hat{\theta} = \frac{\left[W_0 \left(-\left(\frac{q_n^{(c)}h_n f_n}{N_0} + 1\right)e^{-\left(\frac{f_n \ln 2}{B\epsilon e^\epsilon} + 1\right)} + \frac{f_n \ln 2}{B\epsilon e^\epsilon} + 1\right) \ln 2\right]}{B} + \frac{1}{s_n}.$$

Proof: Based on (20a), for $R_n^* = 1$, it can be derived that $\frac{N_0 \ln 2}{Bh_n} 2^{\frac{\ell_n^{(s)}}{Bt_n^*}} - \left(q_n^{(c)} + \frac{\bar{\lambda}^*}{f_n}\right) \epsilon e^\epsilon < 0$. Combining it with the optimal conditions, $t_n^* = T - \frac{\ell_n^{(s)}}{s_n}$, and $\lambda^* = \frac{N_0}{h_n} \left[2^{\frac{\ell_n^{(s)}}{Bt_n^*}} \left(\frac{\ell_n^{(s)} \ln 2}{Bt_n^*} - 1 \right) + 1 \right]$, leads to the desired result. \square

Lemma 5 shows that the optimal decision on compress-or-not has a *threshold-based* structure. To be specific, data compression is preferred only if the sensing-data size exceeds a threshold depending on the channel gain and compression power among others. This is due to the fact that reducing data sizes by compression can substantially lower the exponentially-increasing energy required for transmitting large amounts of data.

Based on the conditions in (20a)-(20c), the key results of this subsection are derived and stated in the following proposition.

Proposition 4 (Optimal Compression and Transmission). The solution of P1-B is as follows.

- 1) The optimal sensor-transmission durations $\{t_n^*\}$ are

$$t_n^* = T - \frac{\ell_n^{(s)} (e^{\epsilon R_n^*} - e^\epsilon)}{f_n} - \frac{\ell_n^{(s)}}{s_n}, \quad \forall n, \quad (21)$$

which corresponds to full utilization of the crowd-sensing duration.

- 2) The optimal compression ratios $\{R_n^*\}$ are

$$R_n^* = \max \left\{ \min \left\{ \hat{R}_n, R_{\max} \right\}, 1 \right\}, \quad \forall n, \quad (22)$$

where \hat{R}_n satisfies: $z(\hat{R}_n) = 0$ with the function $z(R_n)$ defined by

$$z(R_n) = \left[q_n^{(c)} - \frac{1}{h_n f_n} g \left(\frac{1}{d(R_n) R_n} \right) \right] \epsilon e^{\epsilon R_n} - \frac{1}{h_n R_n^2} f' \left(\frac{1}{d(R_n) R_n} \right), \quad (23)$$

$$\text{and } d(R_n) \triangleq \frac{T}{\ell_n^{(s)}} - \frac{1}{s_n} - \frac{1}{f_n} C(R_n, \epsilon) > 0.$$

The proof is given in Appendix D. Even though \hat{R}_n has no closed form, it can be computed by the bisection-search method in Algorithm 2. This is due to the monotonicity of function $z(R_n)$ as shown in the lemma below and proved in Appendix E.

Lemma 6. $z(R_n)$ is a *monotone-increasing* function of R_n .

Consequently, the effects of parameters on the optimal compression ratio are detailed below.

Corollary 5 (Properties of Optimal Compression Ratios). The optimal compression ratios $\{R_n^*\}$ have the following properties:

Algorithm 2 Optimal Lossless Compression Ratio Algorithm

- **Step 1** [Initialize]: Let $R_\ell = 1$, $R_h = R_{\max}$, $\varepsilon > 0$. Obtain $z(R_\ell)$ and $z(R_h)$.
 - **Step 2** [Bisection search]: While $z(R_\ell) \neq 0$ and $z(R_h) \neq 0$, update R_ℓ and R_h as follows.
 - (1) Define $R_n^* = (R_\ell + R_h)/2$, compute $z(R_n^*)$.
 - (2) If $z(R_n^*) > 0$, let $R_h = R_n^*$, else $R_\ell = R_n^*$.
 Until $R_h - R_\ell < \varepsilon$.
-

Algorithm 3 Efficient Algorithm for Lossless Compression Solving Problem P1

- **Step 1**: Initialize the compression ratio R_n^* .
 - **Step 2**: Repeat
 - (1) Given fixed compression ratio, find the optimal power allocation P_n^* and the sensing-data size $(\ell_n^{(s)})^*$ by using Algorithm 1.
 - (2) Given fixed sensing-data size, update the compression ratio R_n^* by using Algorithm 2.
 Until convergence or a maximum number of iterations has been reached.
-

- 1) If the compression powers $\{q_n^{(c)}\}$ are identical but the channel gains satisfy $h_1 \geq h_2 \cdots \geq h_N$, then $R_1^* \leq R_2^* \cdots \leq R_N^*$.
- 2) If the channel gains $\{h_n\}$ are identical but the compression powers satisfy $q_1^{(c)} \geq q_2^{(c)} \cdots \geq q_N^{(c)}$, then $R_1^* \leq R_2^* \cdots \leq R_N^*$.

Proposition 5 is proved in Appendix F. Accordingly, it is more energy-efficient for a sensor to perform more aggressive compression in the case of a poor channel or small compression-power consumption.

E. Complexity Analysis

Combing the results in the preceding subsections, the efficient control policy for achieving the maximum operator's reward can be computed by an iterative procedure summarized in Algorithm 3 with the complexity analyzed as follows. In the outer iteration, the algorithm alternatively optimizes the control policy given fixed compression ratios and sensing-data sizes. First, given fixed compression ratios, the optimal control policy can be computed by the one-dimensional search for λ^* described in Algorithm 1, which invokes an inner iteration. The complexity of the one-dimensional search can be represented by $\mathcal{O}(\log(1/\varepsilon))$ given a solution accuracy $\varepsilon > 0$. Moreover, the complexity for the sensor-transmission, power-allocation, and

sensing-data size is $\mathcal{O}(N)$ in each inner iteration. Hence, the total complexity of the control policy given fixed compression ratios is $\mathcal{O}(N \log(1/\varepsilon))$. Next, given fixed sensing-data sizes, the optimal compression ratio for each sensor can be computed by another one-dimensional search in Algorithm 2. Therefore, each iteration also has the computation complexity $\mathcal{O}(N \log(1/\varepsilon))$. Last, the complexity of the outer iteration can be characterized by $\mathcal{O}(\log(1/\varepsilon))$. In summary, the total complexity for Algorithm 3 is $\mathcal{O}(N \log^2(1/\varepsilon))$, which is feasible in practical systems.

IV. EXTENSION TO LOSSY COMPRESSION

The preceding section considers lossless compression. Its results are extended in this section to the case of lossy compression. To this end, problem P1 is modified to include the quality factor $b_n = \frac{1}{\sqrt{R_n}}$ for lossy compression, leading to its lossy-compression counterpart as follows:

$$\begin{aligned}
 \max_{\substack{\bar{P}_n \geq 0, \bar{\ell}_n^{(s)} \geq 0, \\ \bar{R}_n \in [1, \bar{R}_{\max}], \bar{t}_n \geq 0}} \quad & \sum_{n=1}^N a_n \log \left(1 + \frac{1}{\sqrt{\bar{R}_n}} \bar{\ell}_n^{(s)} \right) - c \sum_{n=1}^N \bar{P}_n T_0 \\
 \text{s.t.} \quad & \sum_{n=1}^N \bar{P}_n \leq P_0, \\
 \text{(P3)} \quad & \frac{\bar{\ell}_n^{(s)}}{s_n} + \frac{\bar{\ell}_n^{(s)}(e^{\bar{\epsilon} \bar{R}_n} - e^{\bar{\epsilon}})}{f_n} + \bar{t}_n \leq T, \quad n = 1, \dots, N, \\
 & q_n^{(r)} \bar{\ell}_n^{(s)} + q_n^{(s)} \bar{\ell}_n^{(s)} + q_n^{(c)} \bar{\ell}_n^{(s)}(e^{\bar{\epsilon} \bar{R}_n} - e^{\bar{\epsilon}}) + \frac{\bar{t}_n}{h_n} f \left(\frac{\bar{\ell}_n^{(s)}}{\bar{R}_n \bar{t}_n} \right) \leq \eta \bar{P}_n h_n T_0, \quad n = 1, \dots, N.
 \end{aligned}$$

Problem P3 has a similar form as P1 and is also non-convex. Leveraging the iterative solution approach developed in the preceding section, problem P3 can be decomposed into two sub-problems for optimizing two corresponding subsets of parameters, $\{P_n, \ell_n^{(s)}, t_n\}$ and $\{R_n, \ell_n^{(s)}, t_n\}$. The first sub-problem has the same form as its lossless-compression counterpart, problem P1-A; thus, it can be solved in a similar way (see Section III-C). The second sub-problem (see problem P4 below) differs from P1-B due to the addition of sensing-data sizes $\{\ell_n^{(s)}\}$ to the optimization variables. The reason is that lossy-compression causes information loss and thereby reduces data utility, which has to be compensated for by increasing the sensing-data sizes. To address this issue and also for tractability, we apply the constraint that the data utility contributed by different sensors is fixed in problem P4 as $\{u_n\}$, which results from solving the first sub-problem. Consequently, problem P4 follows from the master problem P3 as:

$$\text{(Data utility constraint)} \quad u_n = b_n \bar{\ell}_n^{(s)} = \frac{1}{\sqrt{\bar{R}_n}} \bar{\ell}_n^{(s)}. \quad (24)$$

Then the corresponding optimization problem can be formulated as follows.

$$\begin{aligned}
 \min_{\bar{R}_n \in [1, \bar{R}_{\max}], \bar{t}_n \geq 0, \bar{\ell}_n^{(s)} \geq 0} \quad & \bar{\ell}_n^{(s)} \left[q_n^{(r)} + q_n^{(s)} + q_n^{(c)} \left(e^{\bar{\epsilon} \bar{R}_n} - e^{\bar{\epsilon}} \right) \right] + \frac{\bar{t}_n}{h_n} f \left(\frac{\bar{\ell}_n^{(s)}}{\bar{R}_n \bar{t}_n} \right) \\
 \text{(P4)} \quad \text{s.t.} \quad & \frac{1}{\sqrt{\bar{R}_n}} \bar{\ell}_n^{(s)} = u_n, \quad n = 1, \dots, N, \\
 & \bar{t}_n + \frac{\bar{\ell}_n^{(s)}}{s_n} + \frac{\bar{\ell}_n^{(s)}}{f_n} \left(e^{\bar{\epsilon} \bar{R}_n} - e^{\bar{\epsilon}} \right) \leq T, \quad n = 1, \dots, N.
 \end{aligned}$$

This problem is solved in the following sub-section.

A. Joint Optimization of Sensing-Data Sizes, Compression, and Transmission

Problem P4 can be shown to be a non-convex problem but may be transformed into a convex problem as follows. Here we define a set of new variables $\{r_n\}$ as $r_n = \sqrt{\bar{R}_n} \in [1, r_{\max}]$ where $r_{\max} = \sqrt{\bar{R}_{\max}}$. Hence, $\bar{\ell}_n^{(s)} = u_n r_n$ and $\bar{R}_n = r_n^2$. Substituting them into problem P4 gives:

$$\begin{aligned}
 \min_{r_n \in [1, r_{\max}], \bar{t}_n \geq 0} \quad & u_n r_n \left[q_n^{(r)} + q_n^{(s)} + q_n^{(c)} \left(e^{\bar{\epsilon} r_n^2} - e^{\bar{\epsilon}} \right) \right] + \frac{\bar{t}_n}{h_n} f \left(\frac{u_n}{\bar{t}_n r_n} \right) \\
 \text{(P5)} \quad \text{s.t.} \quad & \bar{t}_n + u_n r_n \left(\frac{1}{s_n} + \frac{e^{\bar{\epsilon} r_n^2} - e^{\bar{\epsilon}}}{f_n} \right) \leq T, \quad n = 1, \dots, N.
 \end{aligned}$$

Using a similar approach as that for deriving Lemma 4, it can be proved that problem P5 is a convex optimization problem. Then applying the Lagrange method as for solving problem P1-B, the key results of this subsection are derived, as stated in the following corollary.

Proposition 5 (Optimal Lossy Compression and Transmission). The solution of P5 is as follows.

- 1) The optimal sensor-transmission durations $\{\bar{t}_n^*\}$ are

$$\bar{t}_n^* = T - \frac{u_n r_n^* \left(e^{\bar{\epsilon} r_n^{*2}} - e^{\bar{\epsilon}} \right)}{f_n} - \frac{u_n r_n^*}{s_n}, \quad \forall n, \quad (25)$$

which corresponds to full utilization of the crowd-sensing duration.

- 2) The optimal square roots of compression ratios $\{r_n^*\}$ are

$$r_n^* = \max \{ \min \{ \hat{r}_n, r_{\max} \}, 1 \}, \quad \forall n, \quad (26)$$

where \hat{r}_n satisfies: $z(\hat{r}_n) = 0$ with the function $z(r_n)$ defined by

$$\bar{z}(r_n) = r_n Q'(r_n) + Q(r_n) - \frac{1}{h_n} g \left(\frac{1}{\bar{d}(r_n) r_n} \right) (V(r_n) + r_n V'(r_n)) - \frac{1}{h_n r_n^2} f' \left(\frac{1}{\bar{d}(r_n) r_n} \right) = 0, \quad (27)$$

where $\bar{d}(r_n) = \frac{T}{u_n} - r_n \left(\frac{1}{s_n} + \frac{e^{\bar{\epsilon} r_n^2} - e^{\bar{\epsilon}}}{f_n} \right)$, $Q(r_n) = q_n^{(r)} + q_n^{(s)} + q_n^{(c)} \left(e^{\bar{\epsilon} r_n^2} - e^{\bar{\epsilon}} \right)$, and $V(r_n) = \left(\frac{1}{s_n} + \frac{e^{\bar{\epsilon} r_n^2} - e^{\bar{\epsilon}}}{f_n} \right)$.

This proposition can be proved by a similar method as that for deriving Proposition 4. Even though \hat{r}_n has no closed form, it can be computed by the bisection method due to the monotonicity of function $\bar{z}(r_n)$ shown in the lemma below, which is proved in Appendix G.

Lemma 7. $\bar{z}(r_n)$ is a *monotone-increasing* function of r_n .

Following a similar approach as that for deriving Corollary 5, it can be proved that the optimal compression ratio increases with the channel gain and decreases with the compression power.

Remark 3 (Lossy versus Lossless Compression). Given the same sensing-data size and compression ratio, as compared to lossless compression, the lossy operation consumes less energy for compression and results in smaller size of compressed data, which further reduces transmission-energy consumption. The disadvantage, however, is that it sacrifices part of data utility due to information loss. Hence, there exists a tradeoff between the energy consumption and data utility for lossy compression. The decision on choosing lossless-or-lossy compression is intractable due to the lack of closed-form expression for the maximum reward (see Proposition 4 and Corollary 5). However, it can be observed that lossy compression is preferred under the following conditions: the channel is poor, compression power is large, or sensing power is small. In these cases, lossy compression can achieve significant energy savings.

V. SIMULATIONS AND DISCUSSION

Simulation parameters are set as follows unless specified otherwise. The WPCS system comprises 1 AP and 10 MSs where the AP transfers wireless power to MSs in the time duration $T_0 = 1$ s. The channels $\{h_n\}$ are modeled as independent Rayleigh fading with average signal attenuation set as 10^{-3} . The bandwidth $B_n = 10$ KHz and the variance of complex-white-Gaussian-channel noise $N_0 = 10^{-9}$ W. For the system reward, the utility weights for all the MSs are the same: $a_n = 0.04$ and the cost weight $c = 0.6$. For each MS, the sensing rate follows a uniform distribution with $s_n \in [1, 10] \times 10^4$ bit/s and energy consumption per bit is uniformly distributed by $q_n^{(s)} \in [1, 10] \times 10^{-12}$ J/bit [37]. For the data compression, the required number of CPU cycles per bit, CPU-cycle frequency, and energy consumption per cycle follow the uniform distribution with $C_n \in [0, 3000]$ cycles/bit, $f_n \in [0.1, 1]$ GHz, and $q_n^{(c)} \in [1, 10] \times 10^{-14}$ J/bit, respectively. In addition, the energy reward per bit is uniformly distributed as: $q_n^{(r)} \in [1, 10] \times 10^{-12}$ J/bit. The maximum compression ratios for lossless and lossy compression are set as $R_{\max} = 3$ and $\bar{R}_{\max} = 25$ with $\epsilon = 4$ and $\bar{\epsilon} = 0.1$, respectively.

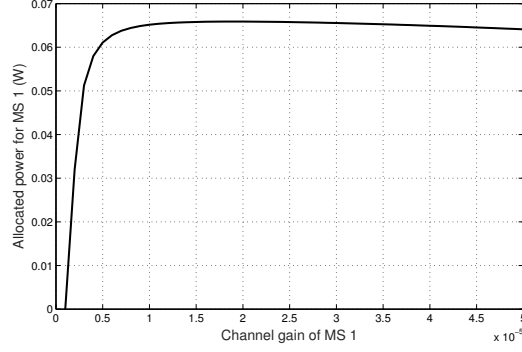


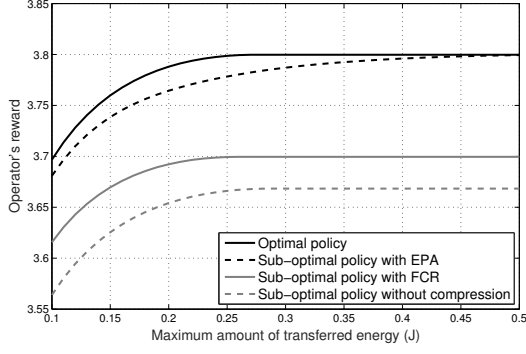
Figure 4: Effects of channel gain on allocated wireless power for a particular sensor while channel gains of other sensors are fixed at 10^{-5} .

A. Wireless Power Allocation

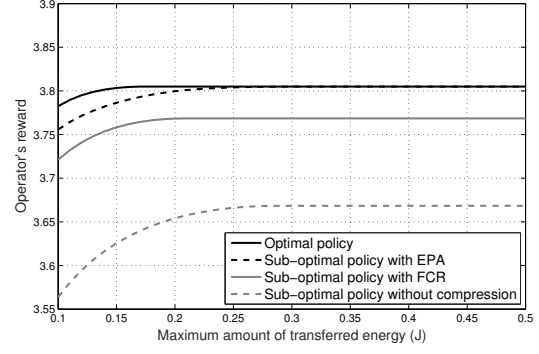
Numerical results computed by using Proposition 2 are presented in Fig. 4 for providing insight into the optimal policy for wireless-power allocation. The channel gain of sensor 1 varies while those of sensors $2, \dots, N$ are fixed as 10^{-5} . One can observe that if the channel is poor, sensor 1 does not receive wireless power due to the small priority function. Otherwise, if the channel gain exceeds a threshold (of about 10^{-6}), the allocated wireless power is firstly increasing and then decreasing with the growth of the channel gain. This interesting observation indicates that *when the channel gain is not sufficiently large, the sensor should receive enough power for increasing its data utility*. However, equipped with a good channel, the sensor can contribute to large data utility even with smaller receive power, which allows for saving more power for other sensors in order to increase the sum data utility.

B. WPCS Performance

Three baseline policies are considered for performance comparison. The first one is the *sub-optimal policy with fixed compression ratio* (FCR) that jointly optimizes the power allocation, sensor transmission, and sensing-data size by using the approach in Section III-C. Specifically, the compression ratios for lossless and lossy compression are set as $R_n = 1.5$ and $\bar{R}_n = 4$, respectively, which can achieve the maximum operator's reward for the sub-optimal policy with FCR. The second one is the *sub-optimal policy with equal power allocation* (EPA), which jointly optimizes the sensor transmission, sensing-data size, and compression ratio given the power allocation policy. The third one is the *sub-optimal policy without compression*, which can be regarded as the special case of FCR with the compression ratio set as zero.

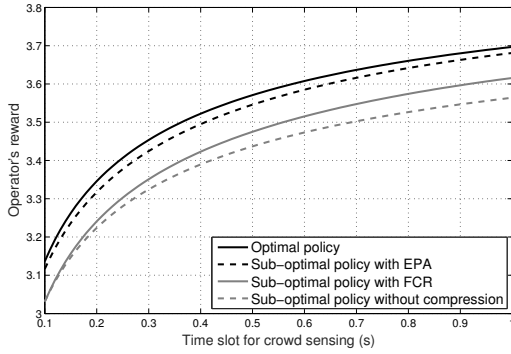


(a) Lossless compression

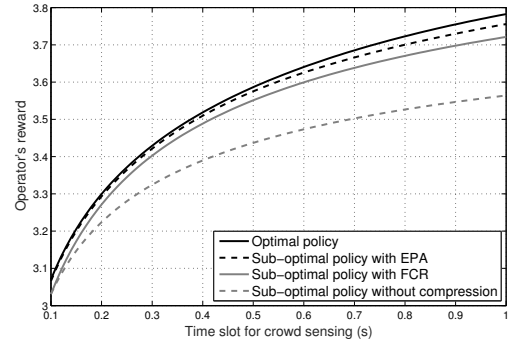


(b) Lossy compression

Figure 5: Operator's reward versus the maximum amount of transferred energy.



(a) Lossless compression



(b) Lossy compression

Figure 6: Operator's reward versus the time slot for crowd sensing.

The curves for the operator's reward versus the maximum amount of transferred energy are displayed in Fig. 5, with the time duration for crowd sensing set as $T = 1$ s. For lossless compression, it can be observed from Fig. 5(a) that the operator's reward for the optimal policy is monotone-increasing with the growth of transferred energy in the small transferred-energy regime. However, when the amount of energy exceeds a threshold (of about 0.25 J), the performance cannot be improved further by simply increasing the transferred energy. The reason is that the bottleneck in this case is no longer energy but other settings such as crowd-sensing duration. Note that *the optimal policy has significant performance gain over the policy with FCR and without compression*, even when the maximum amount of transferred energy is sufficient. This shows the necessity of optimizing the compression ratios to improve system performance when the transferred energy is sufficient. In addition, among the three baseline policies, *the one with EPA has the largest operator's reward among others and approaches close-to-optimal*

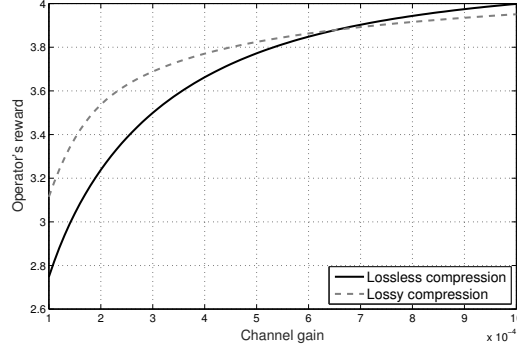


Figure 7: Operator's reward versus channel gain.

performance in the large transferred energy regime. This is due to the fact that optimizing compression ratios can substantially reduce transmission energy consumption, thus allowing for using more energy to sense data for better data utility. For lossy compression, one can observe from Fig. 5(b) that the optimal policy yields larger and comparable operator's reward as compared with the lossless counterpart for the case of small and large transferred energy, respectively. Other observations are similar to those in Fig. 5(a).

Fig. 6 shows the curves for the operator's reward versus the crowd-sensing duration for both compression methods. One can observe from Fig. 6(a) that for lossless compression, the operator's reward is monotone-increasing with the extension of crowd-sensing duration, as it can reduce transmission-energy consumption so as to save more energy for data sensing. However, the growth rate of the operator's reward slows down with the crowd-sensing duration. It indicates that *extending a small crowd-sensing duration can substantially increase the operator's reward.* Moreover, in large crowd-sensing duration regime, lossy compression yields higher operator's reward than in the lossless case. Other observations are similar to those in Fig. 5.

Last, the impact of channel gain on the compression method selection is evaluated in Fig. 7. Several observations are made as follows. First, the operator's reward is observed to be a monotone-increasing function of the channel gain. Next, *lossy and lossless compression is preferred for relatively small and large channel gains, respectively.* The reason is that for poor channels, transmission-energy can dominate other components (e.g., sensing), and it can be substantially reduced by lossy compression due to efficient data-compression performance. Nevertheless, when the channel is good enough, lossless compression can contribute to larger data utility with small compression energy, and thereby may be preferred over the lossy operation..

VI. CONCLUDING REMARKS

This work proposes a multiuser WPCS system and investigates the joint control of power allocation, sensing, compression, and transmission for maximizing the operator's reward. It offers several insights into the control policies of the operator and MSs. To be specific, for the operator, we show that it should select the MSs for participating in the crowd sensing based on its configuration and the individual parameters of MSs. In addition, the optimal power allocation policy has a threshold-based structure depending on a derived crowd sensing priority function. For MSs, each selected sensor should control its compression ratio, sensor transmission, and sensing-data size for minimizing the resultant energy consumption. This work can be further extended to other interesting scenarios such as cooperation among multiple operators and online control of multiuser WPCS systems.

APPENDIX

A. Proof of Lemma 2

This lemma can be proved by contradiction. First, assume that $\left\{ \left(\ell_n^{(s)} \right)^*, t_n^*, P_n^* \right\}$ is the optimal solution satisfying $\alpha_n \left(\ell_n^{(s)} \right)^* + \frac{t_n^*}{h_n} f \left(\frac{\left(\ell_n^{(s)} \right)^*}{R_n t_n^*} \right) < \eta P_n^* h_n T_0$. Then, there exists another feasible power allocation policy, denoted by $P_n^{(1)}$, which satisfies $P_n^{(1)} < P_n^*$ and $\alpha_n \left(\ell_n^{(s)} \right)^* + \frac{t_n^*}{h_n} f \left(\frac{\left(\ell_n^{(s)} \right)^*}{R_n t_n^*} \right) = \eta P_n^{(1)} h_n T_0$. It leads to the following

$$\sum_{n=1}^N a_n \log(1 + (\ell_n^{(s)})^*) - c \sum_{n=1}^N P_n^{(1)} T_0 > \sum_{n=1}^N a_n \log(1 + (\ell_n^{(s)})^*) - c \sum_{n=1}^N P_n^* T_0,$$

which contradicts the optimality. Similarly, if the optimal solution leads to $\beta_n \left(\ell_n^{(s)} \right)^* + t_n^* < T$, then there exists another feasible policy with $(\ell_n^{(s)})^{(1)}$ that satisfies $(\ell_n^{(s)})^{(1)} = \frac{T - t_n^*}{\beta_n} > \left(\ell_n^{(s)} \right)^*$.

This new policy yields larger operator's reward as

$$\sum_{n=1}^N a_n \log(1 + (\ell_n^{(s)})^{(1)}) - c \sum_{n=1}^N P_n^* T_0 > \sum_{n=1}^N a_n \log(1 + (\ell_n^{(s)})^*) - c \sum_{n=1}^N P_n^* T_0,$$

thus contradicting the assumption. Combining the above together leads to the desired results.

B. Proof of Corollary 1

From (14), the utility weight can be expressed as:

$$a_n = \frac{(\lambda^* + c) N_0 [\beta_n + (T - t_n^*)]}{\eta h_n^2} \left[\left(\frac{T \ln 2}{B R_n \beta_n t_n^*} - 1 \right) e^{\frac{T \ln 2}{B R_n \beta_n t_n^*} - \frac{\ln 2}{B R_n \beta_n}} + \frac{\alpha_n h_n}{N_0 \beta_n} + 1 \right].$$

Given $a_1 < a_2$, it can be directly observed from the above equation that $t_1 > t_2$. As for channel gain, it should satisfy the following equation:

$$h_n \left[\frac{a_n \eta h_n}{(\lambda^* + c) N_0 [\beta_n + (T - t_n^*)]} - \frac{\alpha_n}{N_0 \beta_n} \right] = \left(\frac{T \ln 2}{B R_n \beta_n t_n^*} - 1 \right) e^{\frac{T \ln 2}{B R_n \beta_n t_n^*} - \frac{\ln 2}{B R_n \beta_n}} + 1. \quad (28)$$

Note that both the right hand-side of (28) and $N_0 [\beta_n + (T - t_n^*)]$ are decreasing with t_n . It means that if $h_1 < h_2$, it should satisfy that $t_1 \geq t_2$, thus completing the proof.

C. Proof of Proposition 2

First, combining $\alpha_n \left(\ell_n^{(s)} \right)^* + \frac{t_n^*}{h_n} f \left(\frac{\left(\ell_n^{(s)} \right)^*}{R_n t_n} \right) = \eta P_n^* h_n T_0$ and $\beta_n \left(\ell_n^{(s)} \right)^* + t_n^* = T$ gives

$$P_n^* = \frac{1}{h_n \eta T_0} \left[\frac{t_n^*}{h_n} f \left(\frac{T - t_n^*}{R_n \beta_n t_n^*} \right) + \frac{\alpha_n (T - t_n^*)}{\beta_n} \right].$$

Next, the first and second derivative of P_n are calculated as follows.

$$\frac{\partial P_n}{\partial t_n} = \frac{N_0}{\eta h_n^2 T_0} \left[\left(1 - \frac{T \ln 2}{B R_n \beta_n t_n} \right) 2^{\frac{T - t_n}{B R_n \beta_n t_n}} - 1 \right] - \frac{\alpha_n}{\eta \beta_n h_n}, \quad \frac{\partial^2 P_n}{\partial t_n^2} = \frac{N_0 (T \ln 2)^2}{\eta T_0 (h_n B R_n \beta_n)^2 t_n^3} 2^{\frac{T - t_n}{B R_n \beta_n t_n}}.$$

It can be observed that $\frac{\partial^2 P_n}{\partial t_n^2} > 0$ for $0 \leq t_n \leq T$. Hence $\frac{\partial P_n}{\partial t_n}$ is monotone-increasing for $0 \leq t_n \leq T$ and

$$\left(\frac{\partial P_n}{\partial t_n} \right)_{\max} = \frac{\partial P_n}{\partial t_n} \Big|_{t_n=T} = -\frac{N_n \ln 2}{\eta h_n^2 B R_n \beta_n} - \frac{\alpha_n}{\eta \beta_n h_n} < 0.$$

It means that P_n is monotone decreasing with t_n and $(P_n)_{\min} = P_n|_{t_n=T} = 0$. Combining (13a) and $0 \leq t_n \leq T$ yields

$$\lambda^* > \frac{\frac{a_n}{\beta_n + (T - t_n^*)}}{\frac{\alpha_n}{\eta h_n \beta_n} - \frac{N_0}{\eta h_n^2} \left[\left(1 - \frac{T \ln 2}{B R_n \beta_n t_n^*} \right) 2^{\frac{T - t_n^*}{B R_n \beta_n t_n^*}} - 1 \right]} - c = \frac{a_n \eta h_n}{q_n^{(r)} + q_n^{(s)} + q_n^{(c)} e^{\epsilon R_n} + \frac{N_0 \ln 2}{h_n B R_n}} - c = \varphi_n.$$

If $\lambda^* < \varphi_n$, the optimal sensing time will violate the time constraint $t_n^* > T$; thus the sensor will not be selected and no power will be allocated to it, i.e., $P_n = 0$, which completes the proof.

D. Proof of Proposition 4

Based on (20c), at least one of the two equations $\hat{\lambda}^* = 0$ or $t_n^* + \frac{\ell_n^{(s)}(e^{\epsilon R_n^*} - e^\epsilon)}{f_n} + \frac{\ell_n^{(s)}}{s_n} - T = 0$ should be satisfied. Assume that $t_n^* + \frac{\ell_n^{(s)}(e^{\epsilon R_n^*} - e^\epsilon)}{f_n} + \frac{\ell_n^{(s)}}{s_n} - T \neq 0$, then it has $\hat{\lambda}^* = 0$, which leads to $R_n^* \rightarrow \infty$ according to (20b). This, however, contradicts the finite compression ratio. Hence, it should satisfy: $t_n^* + \frac{\ell_n^{(s)}(e^{\epsilon R_n^*} - e^\epsilon)}{f_n} + \frac{\ell_n^{(s)}}{s_n} = T$. The optimal solution should satisfy (20a), i.e.,

$$\left(q_n^{(c)} + \frac{\hat{\lambda}^*}{f_n} \right) \epsilon e^{\epsilon R_n^*} - \frac{1}{h_n (R_n^*)^2} f' \left(\frac{\ell_n^{(s)}}{t_n^* R_n^*} \right) = 0.$$

Combining the above with the optimal conditions, $\hat{\lambda}^* = -\frac{1}{h_n} g \left(\frac{\ell_n^{(s)}}{t_n^* R_n^*} \right)$ and $t_n^* = T - \frac{\ell_n^{(s)}(e^{\epsilon R_n^*} - e^\epsilon)}{f_n} - \frac{\ell_n^{(s)}}{s_n}$ according to (20b) and (20c), produces the desired result.

E. Proof of Lemma 6

The first derivative of function $z(R_n)$ is

$$\begin{aligned} \frac{\partial z(R_n)}{\partial R_n} &= \frac{N_0 \ln 2}{BR_n^2 h_n} \left[\frac{2}{R_n} + \frac{\ln 2 [R_n d(R_n)]'}{B [R_n d(R_n)]^2} \left(1 - \frac{R_n d'(R_n)}{d(R_n)} \right) \right] e^{\frac{\ln 2}{BR_n d(R_n)}} \\ &\quad + \left[q_n^{(c)} - \frac{1}{h_n f_n} g \left(\frac{1}{d(R_n) R_n} \right) \right] \epsilon^2 e^{\epsilon R_n}. \end{aligned}$$

First, it has $[R_n d(R_n)]' = d(R_n) - R_n d'(R_n)$. Hence, $[R_n d(R_n)]' > 0$ when $d(R_n) > R_n d'(R_n)$, and $[R_n d(R_n)]' < 0$ when $d(R_n) < R_n d'(R_n)$. Combining these together leads to

$$\frac{\ln 2 [R_n d(R_n)]'}{B [R_n d(R_n)]^2} \left(1 - \frac{R_n d'(R_n)}{d(R_n)} \right) > 0, \quad \text{for } R_n \in [1, R_{\max}].$$

Next, the first derivative of function $g(x)$ can be obtained as

$$g'(x) = -x f''(x) = -\frac{N_0 \ln 2^2}{B^2} 2^{\frac{x}{B}} < 0, \quad \text{for } x > 0.$$

It means that $g(x)$ is monotone-decreasing with x and thus $g(x) \leq g(x)|_{x=0} = 0$ for $x > 0$. Since $\frac{1}{d(R_n) R_n} > 0$, it has $\left[q_n^{(c)} - \frac{1}{h_n f_n} g \left(\frac{1}{d(R_n) R_n} \right) \right] > 0$ for $x > 0$. Combining the above considerations leads to $\frac{\partial z(R_n)}{\partial R_n} > 0$ for $R_n \in [1, R_{\max}]$, thus completing the proof.

F. Proof of Corollary 5

Define a function $\varphi(R_n)$ as $\varphi(R_n) = q_n^{(c)} h_n$. According to (27), it has

$$\varphi(R_n) = q_n^{(c)} h_n = \frac{1}{f_n} g \left(\frac{1}{d(R_n) R_n} \right) + \frac{1}{R_n^2 \epsilon e^{\epsilon R_n}} f' \left(\frac{1}{d(R_n) R_n} \right).$$

The derivation of $\varphi(R_n)$ is

$$\frac{\partial \varphi(R_n)}{\partial R_n} = -\frac{N_0 \ln 2}{BR_n^2 \epsilon e^{\epsilon R_n}} \left[\frac{2 + \epsilon}{R_n \epsilon e^{\epsilon R_n}} + \frac{\ln 2 [R_n d(R_n)]'}{B [R_n d(R_n)]^2} \left(1 - \frac{R_n \epsilon e^{\epsilon R_n}}{f_n d(R_n)} \right) \right] e^{\frac{\ln 2}{BR_n d(R_n)}}.$$

Since $\frac{\ln 2 [R_n d(R_n)]'}{B [R_n d(R_n)]^2} \left(1 - \frac{R_n \epsilon e^{\epsilon R_n}}{f_n d(R_n)} \right)$ is always positive as proved in Appendix E, the function $\varphi(R_n)$ is monotone-decreasing for $R_n \in [1, R_{\max}]$. Given $q_1^{(c)} > q_2^{(c)}$, it can be derived that $R_1 < R_2$. Using a similar approach, it can be proved that $R_1 < R_2$ when $h_1 > h_2$, thus completing the proof.

G. Proof of Lemma 7

The first derivative of $\bar{z}(r_n)$ is

$$\begin{aligned} \frac{\partial \bar{z}(r_n)}{\partial r_n} &= \frac{N_0 \ln 2}{B h_n r_n^2} \left[\frac{2}{r_n} + \frac{\ln 2 [r_n \bar{d}(r_n)]'}{B [r_n \bar{d}(r_n)]^2} \left(1 - \frac{r_n \bar{d}'(r_n)}{\bar{d}(r_n)} \right) \right] e^{\frac{\ln 2}{B r_n \bar{d}(r_n)}} \\ &\quad + (6 + 4\epsilon r_n^2) r_n q_n^{(c)} \epsilon e^{\epsilon r_n^2} - g \left(\frac{1}{\bar{d}(r_n) r_n} \right) \frac{(6 + 4\epsilon r_n^2) \epsilon r_n}{h_n f_n} e^{\epsilon r_n^2}. \end{aligned}$$

The derivative of function $r_n \bar{d}(r_n)$ is $\bar{d}(r_n) - r_n \bar{d}'(r_n)$. Since $[r_n \bar{d}(r_n)]' > 0$ when $\bar{d}(r_n) > r_n \bar{d}'(r_n)$, and $[r_n \bar{d}(r_n)]' < 0$ when $\bar{d}(r_n) < r_n \bar{d}'(r_n)$, then the item $\frac{\ln 2 [r_n \bar{d}(r_n)]'}{B [r_n \bar{d}(r_n)]^2} \left(1 - \frac{r_n \bar{d}'(r_n)}{\bar{d}(r_n)}\right)$ is always positive. Moreover, $g(x) < 0$ when $x > 0$ according to Appendix E. Since $\frac{1}{\bar{d}(r_n) r_n} > 0$, the item $\left[(6 + 4\epsilon r_n^2) r_n q_n^{(c)} \epsilon e^{\epsilon r_n^2} - g\left(\frac{1}{\bar{d}(r_n) r_n}\right) \frac{(6 + 4\epsilon r_n^2) \epsilon r_n}{h_n f_n} e^{\epsilon r_n^2}\right]$ is always positive. Hence $\frac{\partial \bar{Z}(r_n)}{\partial r_n} > 0$ for $r_n \in [1, r_{\max}]$, thus completing the proof.

REFERENCES

- [1] I. F. Akyildiz, W. Su, Y. Sankarasubramaniam, and E. Cayirci, “Wireless sensor networks: A survey,” *Comput. netw.*, vol. 38, no. 4, pp. 393–422, 2002.
- [2] R. K. Ganti, F. Ye, and H. Lei, “Mobile crowdsensing: Current state and future challenges,” *IEEE Commun. Mag.*, vol. 49, no. 11, pp. 32–39, 2011.
- [3] O. Galinina, K. Mikhaylov, K. Huang, S. Andreev, and Y. Koucheryavy, “Wirelessly powered urban crowd sensing over wearables: Trading energy for data,” [Online]. Available: <https://arxiv.org/pdf/1611.05910.pdf>.
- [4] H. Ma, D. Zhao, and P. Yuan, “Opportunities in mobile crowd sensing,” *IEEE Commun. Mag.*, vol. 52, no. 8, pp. 29–35, 2014.
- [5] V. Petrov, A. Samuylov, V. Begishev, D. Moltchanov, S. Andreev, K. Samouylov, and Y. Koucheryavy, “Vehicle-based relay assistance for opportunistic crowdsensing over narrowband iot (NB-IoT),” *IEEE Internet of Things Journal*, to appear.
- [6] X. Zhang, Z. Yang, W. Sun, Y. Liu, S. Tang, K. Xing, and X. Mao, “Incentives for mobile crowd sensing: A survey,” *IEEE Commun. Surveys Tuts.*, vol. 18, no. 1, pp. 54–67, 2016.
- [7] N. M. Avouris and N. Yiannoutsou, “A review of mobile location-based games for learning across physical and virtual spaces,” *J. Universal Comput. Sci.*, vol. 18, no. 15, pp. 2120–2142, 2012.
- [8] S. He, D. H. Shin, J. Zhang, J. Chen, and P. Lin, “An exchange market approach to mobile crowdsensing: Pricing, task allocation and Walrasian equilibrium,” *IEEE J. Sel. Areas Commun.*, vol. 35, no. 4, pp. 921–934, 2017.
- [9] Z. Feng, Y. Zhu, Q. Zhang, L. M. Ni, and A. V. Vasilakos, “TRAC: Truthful auction for location-aware collaborative sensing in mobile crowdsourcing,” *Proc. IEEE Infocom*, pp. 1231–1239, 2014.
- [10] X. Gan, X. Wang, W. Niu, G. Hang, X. Tian, X. Wang, and J. Xu, “Incentivize multi-class crowd labeling under budget constraint,” *IEEE J. Sel. Areas Commun.*, vol. 35, no. 4, pp. 893–905, 2017.
- [11] L. Duan, T. Kubo, K. Sugiyama, J. Huang, T. Hasegawa, and J. Walrand, “Incentive mechanisms for smartphone collaboration in data acquisition and distributed computing,” in *Proc. IEEE Infocom*, 2012, pp. 1701–1709.
- [12] S. Yang, F. Wu, S. Tang, X. Gao, B. Yang, and G. Chen, “On designing data quality-aware truth estimation and surplus sharing method for mobile crowdsensing,” *IEEE J. Sel. Areas Commun.*, vol. 35, no. 4, pp. 832–847, 2017.
- [13] M. A. Alsheikh, D. Niyato, D. Leong, P. Wang, and Z. Han, “Privacy management and optimal pricing in people-centric sensing,” *IEEE J. Sel. Areas Commun.*, vol. 35, no. 4, pp. 906–920, 2017.
- [14] X. Lu, P. Wang, D. Niyato, D. I. Kim, and Z. Han, “Wireless charging technologies: Fundamentals, standards, and network applications,” *IEEE Commun. Surveys Tuts.*, vol. 18, no. 2, pp. 1413–1452, 2016.
- [15] Y. Zeng, B. Clerckx, and R. Zhang, “Communications and signals design for wireless power transmission,” *IEEE Trans. Commun.*, vol. 65, no. 5, pp. 2264–2290, 2016.
- [16] R. Zhang and C. K. Ho, “MIMO broadcasting for simultaneous wireless information and power transfer,” *IEEE Trans. Wireless Commun.*, vol. 12, no. 5, pp. 1989–2001, 2013.

- [17] P. Popovski, A. M. Fouladgar, and O. Simeone, "Interactive joint transfer of energy and information," *IEEE Trans. Commun.*, vol. 61, no. 5, pp. 2086–2097, 2013.
- [18] B. Gurakan, O. Ozel, J. Yang, and S. Ulukus, "Energy cooperation in energy harvesting communications," *IEEE Trans. Commun.*, vol. 61, no. 12, pp. 4884–4898, 2013.
- [19] C. Zhong, H. A. Suraweera, G. Zheng, I. Krikidis, and Z. Zhang, "Wireless information and power transfer with full duplex relaying," *IEEE Trans. Commun.*, vol. 62, no. 10, pp. 3447–3461, 2014.
- [20] Z. Zheng, L. Song, D. Niyato, and Z. Han, "Resource allocation in wireless powered relay networks: A bargaining game approach," *IEEE Trans. Vehi. Techn.*, vol. 66, no. 7, pp. 6310–6323, 2017.
- [21] A. Abrardo and M. Moretti, "Distributed power allocation for D2D communications underlaying/overlying OFDMA cellular networks," *IEEE Trans. Wireless Commun.*, vol. 16, no. 3, pp. 1466–1479, 2017.
- [22] S. Lee, R. Zhang, and K. Huang, "Opportunistic wireless energy harvesting in cognitive radio networks," *IEEE Trans. Wireless Commun.*, vol. 12, no. 9, pp. 4788–4799, 2013.
- [23] C.-F. Liu, M. Maso, S. Lakshminarayana, C.-H. Lee, and T. Q. Quek, "Simultaneous wireless information and power transfer under different CSI acquisition schemes," *IEEE Trans. Wireless Commun.*, vol. 14, no. 4, pp. 1911–1926, 2015.
- [24] M. Gregori and M. Payaró, "Energy-efficient transmission for wireless energy harvesting nodes," *IEEE Trans. Wireless Commun.*, vol. 12, no. 3, pp. 1244–1254, 2013.
- [25] J. Xu, Y. Zeng, and R. Zhang, "UAV-enabled wireless power transfer: Trajectory design and energy region characterization," [Online]. Available: <https://arxiv.org/pdf/1706.07010.pdf>.
- [26] C. You, K. Huang, and H. Chae, "Energy efficient mobile cloud computing powered by wireless energy transfer," *IEEE J. Sel. Areas Commun.*, vol. 34, no. 5, pp. 1757–1771, 2016.
- [27] L. Xie, Y. Shi, Y. T. Hou, and A. Lou, "Wireless power transfer and applications to sensor networks," *IEEE Wireless Commun.*, vol. 20, no. 4, pp. 140–145, 2013.
- [28] K. W. Choi, L. Ginting, P. A. Rosyady, A. A. Aziz, and D. I. Kim, "Wireless-powered sensor networks: How to realize," *IEEE Trans. Wireless Commun.*, vol. 16, no. 1, pp. 221–234, 2017.
- [29] J. Xu, Z. Zhong, and B. Ai, "Wireless powered sensor networks: Collaborative energy beamforming considering sensing and circuit power consumption," *IEEE Commun. Lett.*, vol. 5, no. 4, pp. 344–347, 2016.
- [30] S. Guo, F. Wang, Y. Yang, and B. Xiao, "Energy-efficient cooperative transmission for simultaneous wireless information and power transfer in clustered wireless sensor networks," *IEEE Trans. Commun.*, vol. 63, no. 11, pp. 4405–4417, 2015.
- [31] K. Han and K. Huang, "Wirelessly powered backscatter communication networks: Modeling, coverage, and capacity," *IEEE Trans. Wireless Commun.*, vol. 16, no. 4, pp. 2548–2561, 2017.
- [32] A. V. D. Ven, "Linux OS data compression options: Comparing behavior," <https://clearlinux.org/blogs/linux-os-data-compression-options-comparing-behavior>, 2017.
- [33] A. P. Chandrakasan, S. Sheng, and R. W. Brodersen, "Low-power CMOS digital design," *IEEE J. Solid-State Circuits*, vol. 27, no. 4, pp. 473–484, 1992.
- [34] C. J. V. den Branden Lambrecht and O. Verscheure, "Perceptual quality measure using a spatiotemporal model of the human visual system," in *Proc. SPIE*, vol. 2668, 1996, pp. 450–461.
- [35] D. Yang, G. Xue, X. Fang, and J. Tang, "Crowdsourcing to smartphones: incentive mechanism design for mobile phone sensing," in *Proc. MobiCom*, 2012, pp. 173–184.
- [36] S. Boyd and L. Vandenberghe, *Convex Optimization*. Cambridge University Press, 2004.
- [37] A. Thiagarajan, L. Ravindranath, H. Balakrishnan, S. Madden, and L. Girod, "Accurate, low-energy trajectory mapping for mobile devices," in *Proc. NSDI*, 2011, pp. 267–280.